Detection of microscopic anisotropy in gray matter and in a novel tissue phantom using double Pulsed Gradient Spin Echo MR

M.E. Komlosh [a,*], F. Horkay [a], R.Z. Freidlin [b], U. Nevo [a], Y. Assaf [c,d], P.J. Basser [a]

[a] *Section on Tissue Biophysics and Biomimetics, NICHD, NIH, Bethesda, MD 20892, USA*
[b] *Computational Bioscience and Engineering Laboratory, Center for Information Technology, National Institutes of Health Bethesda, MD, 20892, USA*
[c] *Department of Neurobiochemistry, George S. Wise Faculty of Life Sciences, Tel Aviv University, 69978, Israel*
[d] *Levie-Edersheim-Gitter Institute for Human Brain Mapping, Tel Aviv Sourasky Medical Center, Tel Aviv University, Tel Aviv 69978, Israel*

Abstract

A double Pulsed Gradient Spin Echo (d-PGSE) MR experiment was used to measure and assess the degree of local diffusion anisotropy in brain gray matter, and in a novel "gray matter" phantom that consists of randomly oriented tubes filled with water. In both samples, isotropic diffusion was observed at a macroscopic scale while anisotropic diffusion was observed at a microscopic scale, however, the nature of the resulting echo attenuation profiles were qualitatively different. Gray matter, which contains multiple cell types and fibers, exhibits a more complicated echo attenuation profile than the phantom. Since microscopic anisotropy was observed in both samples in the low q regime comparable to that achievable in clinical scanner, it may offer a new potential contrast mechanism for characterizing gray matter microstructure in medical and biological applications.
© 2007 Published by Elsevier Inc.

1. Introduction

Diffusion weighted imaging (DWI) is commonly used to characterize normal brain structure and brain pathology [1]. Diffusion tensor MRI (DTI) measurements, in particular, reveal significant differences in the macroscopic structure of gray and white matter. Using DTI, white matter typically appears to be anisotropic and gray matter appears isotropic [2]. This difference can be attributed to differences in the anatomical and architectural organization of these tissues.

White matter consists of highly ordered bundles at the molecular, microscopic, and macroscopic length scales with its parallel structure often exceeding the MRI voxel length scale (Fig. 1d–f). Its macroscopic anisotropic diffusion profile can be adequately characterized by an anisotropic apparent diffusion tensor [3].

Gray matter, on the other hand, has multiple cell types such as neuronal cell bodies and processes, randomly oriented axons, dendritic fibers, oligodendrocytes, extracellular matrices, etc. [4]. While each axonal projection and dendritic fiber has a particular orientation, which may exhibit an anisotropic diffusion profile on a microscopic scale, these neural processes are randomly oriented at the macroscopic voxel length scale (Fig. 1a and b). Thus, the isotropic diffusion tensor that is measured in gray matter is likely the result of powder averaging of the local anisotropic diffusion profiles over a myriad of microdomains [2] (see Fig. 1c).

Although, for macroscopically anisotropic materials like white matter the use of Pulsed Gradient Spin Echo [5,6] based sequences is sufficient to reveal their anisotropy, this sequence fails to detect anisotropy in microscopically anisotropic but macroscopically isotropic materials. For the later case, the use of multi-gradient orientation techniques has been proposed.

---

* Corresponding author. Fax: +1 301 435 5035.
E-mail address: michalk@mail.nih.gov (M.E. Komlosh).
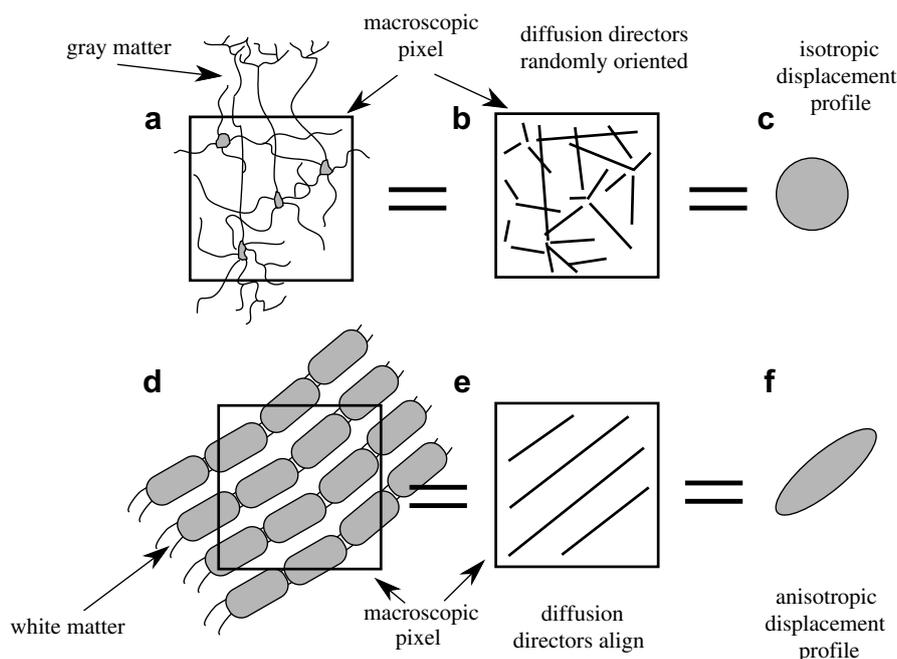
Fig. 1. (a,d) Illustration of gray and white matter tissue with respect to a *macroscopic* pixel. *Note.* MRI pixel length scale is significantly larger than that illustrated. (b,e) The distributions of diffusion directors of the gray and white matter fibers within each pixel. (c,f) The resulting displacement profile averaged over the pixel.

In this work the double Pulsed Gradient Spin Echo (d-PGSE) experiment [7–9] is used to detect or discover whether gray matter exhibits microscopic diffusion anisotropy. The d-PGSE sequence (Fig. 2) and its two-dimensional variants [10] are already well-established techniques in non-medical applications to characterize local anisotropy of macroscopically isotropic materials, such as liquid crystals [7,11] prolate yeast cells [8] and plants [12].

The d-PGSE sequence consists of two single-PGSE blocks, which are concatenated. The resulting spins from the first PGSE block become the population of spins interrogated by the second PGSE block. Because the resulting

echoes depend on the spin evolution in both encoding periods, these contain information about the spins' diffusion histories during both PGSE blocks.

To assess the presence of microscopic diffusion anisotropy, one compares two d-PGSE experiments in which diffusion sensitizing gradients are applied in the same and in orthogonal directions. For microscopically isotropic materials, regardless of the diffusion gradient encoding directions, the resulting echo attenuations all superimpose. However, in the case of materials that exhibit local anisotropy, the resulting curves observed from the collinear and orthogonal diffusion gradient encoding directions do not superimpose. Consequently, a difference between these curves indicates microscopic anisotropy.

To explore the origin of gray matter anisotropy, we also constructed a "gray matter" phantom that is macroscopically isotropic and microscopically anisotropic. The phantom is designed to be stable, so it can also be used as a diffusion standard for calibrating the d-PGSE sequences and NMR hardware. Furthermore, the phantom has a simple geometry so that the displacement history of spins can be mathematically modeled.

2. Materials and methods

2.1. Experimental design

The double-PGSE sequence was applied in nine different combinations of gradient directions between the two pairs of gradient pulses (PGSE blocks). Three collinear directions: X_X, Y_Y and Z_Z; and six orthogonal
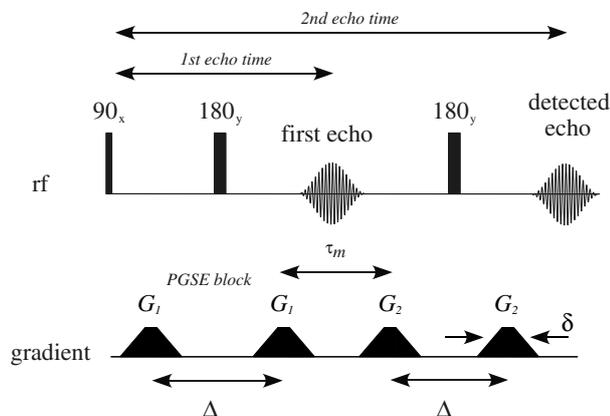
Fig. 2. Double-PGSE pulse sequence. G_1 and G_2 can be either in the same direction (i.e., collinear) or in orthogonal directions. The mixing time, τ_m, is the time between the two d-PGSE blocks.

combinations: *X_Y, Y_X, X_Z, Z_X, Y_Z* and *Z_Y*, were used. Note that combinations like *X_Y* and *Y_X* should yield the same attenuation profile, so differences between them can be used to assess system software and hardware performance. The second echo time was chosen to be different than twice the first echo time to avoid additional spurious echoes, which would result if imperfect 180° RF pulses were refocused at the same time as the d-PGSE echo. The gradient pulses were stepped simultaneously in both PGSE blocks with the same strength and duration. We also repeated the experiment using three polar collinear directions, e.g., *X* and −*X*, to test for possible differences in signal attenuation between collinear and polar collinear directions.

All experiments were performed at a temperature of 20.8 ± 0.1 °C on a 7T vertical Bruker Avance MR imaging system equipped with a Micro2.5 microimaging probe, having a maximum gradient strength of 24.65 mT/m/A in three orthogonal directions with a nominal peak gradient current supply of 60 A per channel. The number of scans varied depending on the amount of signal from each sample.

The sequence was first tested using an isotropic sample of 5 Centistokes polydimethylsiloxane (PDMS) solution (Sigma–Aldrich). This PDMS diffusivity is an order of magnitude lower than that of water, which allows us to use gradient strengths comparable to those used to observe restricted water diffusion. The d-PGSE experiment was preformed with nine gradient combinations using gradient pulse length (δ) = 3 ms, diffusion time (Δ) = 75 ms, 1st echo time = 85 ms, 2nd echo time = 185 ms, the mixing time between the two PGSE blocks (τ_m) = 11.5 ms, number of scans (NS) = 2, and the repetition time (TR) = 4 s. The maximum gradient strength used was 400 mT/m. All the echo attenuation profiles, regardless of gradient combinations, coalesce (data not show) which means that no software and hardware artifacts were observed.

2.2. "Gray matter" phantom

The "gray matter" phantom is a microscopically anisotropic, macroscopically isotropic construct that was prepared from an ensemble of randomly oriented 0.5 mm long fused silica glass tubes with ID = 20 μm and OD = 90 μm (Polymicro Technologies). The tubes were filled with water by condensation of water vapor on the inner walls of the tubes. This process was carried out at a constant vapor pressure, below the saturated vapor pressure of the pure water, ensuring that capillary condensation occured only inside the tubes. The filled tubes were then immersed in deuterated 1,2-di-chloro-benzene (Cambridge Isotope Laboratories, Inc.). Due to density differences between the water and dichlorobenzene, any water molecule that "escapes" the tube is forced to the surface of the sample. This ensures that the only proton signal in the spectrum results from the water inside the tubes. d-PGSE experiments were repeated every few months to ensure stability of the phantom and reproducibility of the

data. To examine the magnetic field homogeneity inside the fused silica tubes, an aligned phantom was constructed, which consists of the same fused silica tubes with ID of 21 μm, OD of 90 μm and length of 1 cm. The tubes were filled with water and surrounded by deuterated dichlorobenzene.

The double-PGSE experiments were performed on the "gray matter" phantom using two sets of acquisition parameters: The first was designed to observe diffusion anisotropy at short diffusion times (Δ) and low gradient strength (G). In this regime anisotropy is observed while the displacement profile of spins is approximately Gaussian. This approximation holds when only a fraction of the spins can "feel" the confining walls of the tube while most of the spins still exhibit free diffusion [13]. The parameters used were: $\delta = 5$ ms, $\Delta = 15$ ms, 1st echo time = 85 ms, 2nd echo time = 180 ms, $\tau_m = 70$ ms, NS = 8 and TR = 4 s. The second set of acquisition parameters was designed to observe restricted diffusion behavior at long diffusion times, where most spins had time to encounter the tube walls, which results in a non-Gaussian displacement profile (i.e., restricted diffusion) of spins. The parameters used were: $\delta = 3$ ms, $\Delta = 75$ ms, 1st echo time = 140 ms, 2nd echo time = 290 ms, $\tau_m = 70$ ms, NS = 32 and TR = 4 s. The maximum gradient strength used in both experiments was 300 mT/m.

Simulations were carried out for the echo attenuations resulting from both diffusion regimes using Eqs. (1a) and (1b), which were derived in [7]

$$E_{Z\_Z}(q) = \int_0^1 \exp[-4\pi^2 q^2 \Delta (2D_\| \cos^2\theta + 2D_\perp \sin^2\theta)]\, d\cos\theta \tag{1a}$$

$$\begin{aligned} E_{Z\_X}(q) = (2\pi)^{-1} \int_0^{2\pi} d\phi \int_0^1 \exp[&-4\pi^2 q^2 \Delta (D_\| \cos^2\theta \\ &+ D_\| \sin^2\theta \cos^2\phi + D_\perp \sin^2\theta + D_\perp \sin^2\phi \\ &+ D_\perp \cos^2\theta \cos^2\phi)]\, d\cos\theta \end{aligned} \tag{1b}$$

$E_{Z\_Z}(q)$ and $E_{Z\_X}(q)$ are the echo attenuations resulting from the d-PGSE experiment. The subscripts Z_Z and Z_X represent the directions of the PGSE blocks, i.e., collinear and orthogonal. $D_\|$ and $D_\perp$ are the parallel and perpendicular diffusivities within the tubes, and $q = (2\pi)^{-1} \gamma G \delta$ where γ is the gyromagnetic ratio and G is the gradient strength. The signal attenuation is an average over all possible tube orientations, θ and ϕ, the polar and azimuthal angles, respectively. The model above is based on the assumption that diffusion is anisotropic at the microscopic scale but its displacement probability is Gaussian, and that these microscopically anisotropic domains are distributed uniformly in all directions. We know of no published model of a d-PGSE experiment that describes restricted diffusion in tubes.

2.3. Biological tissue d-PGSE

Double-PGSE experiments were repeated with a biological specimen consisting of cortical gray matter obtained

from formalin fixed Rhesus monkey brain. The gray matter part of the brain tissue was removed, cut, and immersed in perfluoro polyether (Fomblin, LC/8, Solvay Solexis) to minimize the susceptibility difference between tissue and surrounding. Fomblin is immiscible in water and does not produce a proton signal. In addition the experiment was performed on a slice of white matter taken from a formalin fixed pig spine. This tissue is macroscopically anisotropic and served as a control. The white matter tissue and gray matter were prepared in the same way. To ensure minimum stress on the tissue the specimens were loaded from the bottom into a 5 mm NMR tube sealed at the bottom with a plug (New Era Enterprises, Inc.) and from the top with a 5 mm plunger (Shigemi, Inc.). The susceptibility of both plug and plunger matches that of D_2O. The gray matter sample d-PGSE experiment was carried out with $\delta = 6$ ms and $\Delta = 75$ ms with the 1st echo time = 85 ms and the 2nd echo time = 185 ms, $\tau_m = 17.5$ ms NS = 32 and TR = 4 s. The maximum gradient used in this experiment was 250 mT/m. The white matter sample parameters were with $\delta = 3$ ms and $\Delta = 75$ ms with the 1st echo time = 115 ms and the 2nd echo time = 240 ms, $\tau_m = 45$ ms, NS = 8 and TR = 4 s. The maximum gradient used in this experiment was 400 mT/m. The three polar collinear directions (X_X, Y_Y and Z_Z) d-PGSE experiment were performed on the white matter tissue sample for comparison between the phantom and biological tissue.

2.4. Single-PGSE

Prior to performing the double-PGSE experiment on the phantom and gray matter tissue, a single-PGSE sequence was applied on all samples. This experiment was done to verify the macroscopic nature of the samples, isotropic in the case of the phantom and the cortical tissue, and anisotropic in the case of the white matter, and was preformed using three gradient directions; X, Y and Z. The white matter tissue experimental parameters were $\delta = 5$ ms, $\Delta = 60$ ms, echo time (TE) = 70 ms, NS = 1 and TR = 4 s and maximum gradient strength was 300 mT/m. The phantom experimental parameters were $\delta = 6$ ms, $\Delta = 75$ ms, TE = 85 ms, NS = 1 and TR = 4 s and maximum gradient strength was 400 mT/m. The gray matter cortical tissue parameters were $\delta = 6$ ms, $\Delta = 60$ ms, TE = 70 ms, NS = 1, TR = 4 s and maximum gradient strength was 400 mT/m.

3. Results and discussion

3.1. Single-PGSE

Fig. 3a–c shows PGSE signal attenuations for the "gray matter" phantom, fixed cortical tissue and fixed white matter. The cortical tissue (Fig. 3a) echo attenuations fall on the same curve, regardless of the diffusion gradient direction, indicating macroscopic isotropy. In the "gray matter" phantom (Fig. 3b) slight macroscopic anisotropy can be observed along the Z direction. This small deviation from the X and Y directions might result from the sedimentation process during phantom preparation. In that case, the favorable direction for the tubes to settle would be perpendicular to the main magnetic field, which would cause more restriction in that direction. However this effect is minor and can be seen only in high q values and long diffusion times, thus for our purpose the phantom can be considered macroscopically isotropic. The non-mono-exponential nature of the echo attenuation curves resulting from the single-PGSE experiment of the gray matter specimen and the phantom (Fig. 3a and b) suggests diffusion occurs within impermeable microdomains. Similar behavior was recently observed in [14,15]. However, the coalescence of all curves regardless of their gradient direction indicates that, although spins may encounter impermeable barriers, both samples exhibit a macroscopically isotropic displacement profile, i.e., local anisotropy cannot be detected. Any deviation from that behavior implies macroscopic anisotropy where white matter is a prime example. The white matter (Fig. 3c), whose axis is oriented along the Z-axis, shows the expected macroscopic anisotropic behavior where the echo attenuation resulting from the Z diffusion gradient direction is greater than along the X and Y diffusion gradient directions.

3.2. "Gray matter" phantom d-PGSE

Fig. 4a and b shows the double-PGSE attenuation for the "gray matter" phantom for two different diffusion displacement profile regimes. In both figures local anisotropy is detected since the attenuation profiles of the collinear gradient combination diverge from the orthogonal gradient combination. Fig. 4a shows the echo attenuations using experimental parameters expected to result in an approximately Gaussian displacement distribution (i.e., a short Δ and low gradient strength). In this regime, the tube walls reflect most spins inside the tube, but do not have enough time to sample the entire pore space. The curves generated from Eqs. (1a) and (1b) are consistent with the experimental d-PGSE data using $D_\parallel = 2.05 \times 10^{-3}$ mm^2/s and $D_\perp = 0.76 \times 10^{-3}$ mm^2/s. The value of $D_\parallel$, which corresponds to free diffusion along the tube, agrees with the value for free water diffusion at the temperature of the experiment, which was verified with PGSE experiments. The close fit with the expected diffusion coefficient indicates that in the approximately Gaussian regime the d-PGSE echo attenuations can be represented by a multiplication of two independent PGSE blocks as depicted in Eqs. (1a) and (1b). Fig. 4b on the other hand displays echo attenuation profiles obtained in the restricted regime in which the spins inside the tubes sample the entire pore space (i.e., long Δ, high gradient strength). Here, the diffusion profile no longer can be described adequately by Gaussian displacement distribution. Indeed non-linear curve fitting using Eqs. (1a) and (1b) seems to agree only for low q values using fitted diffusion coefficients of $D_\parallel = 1.47 \times 10^{-3}$
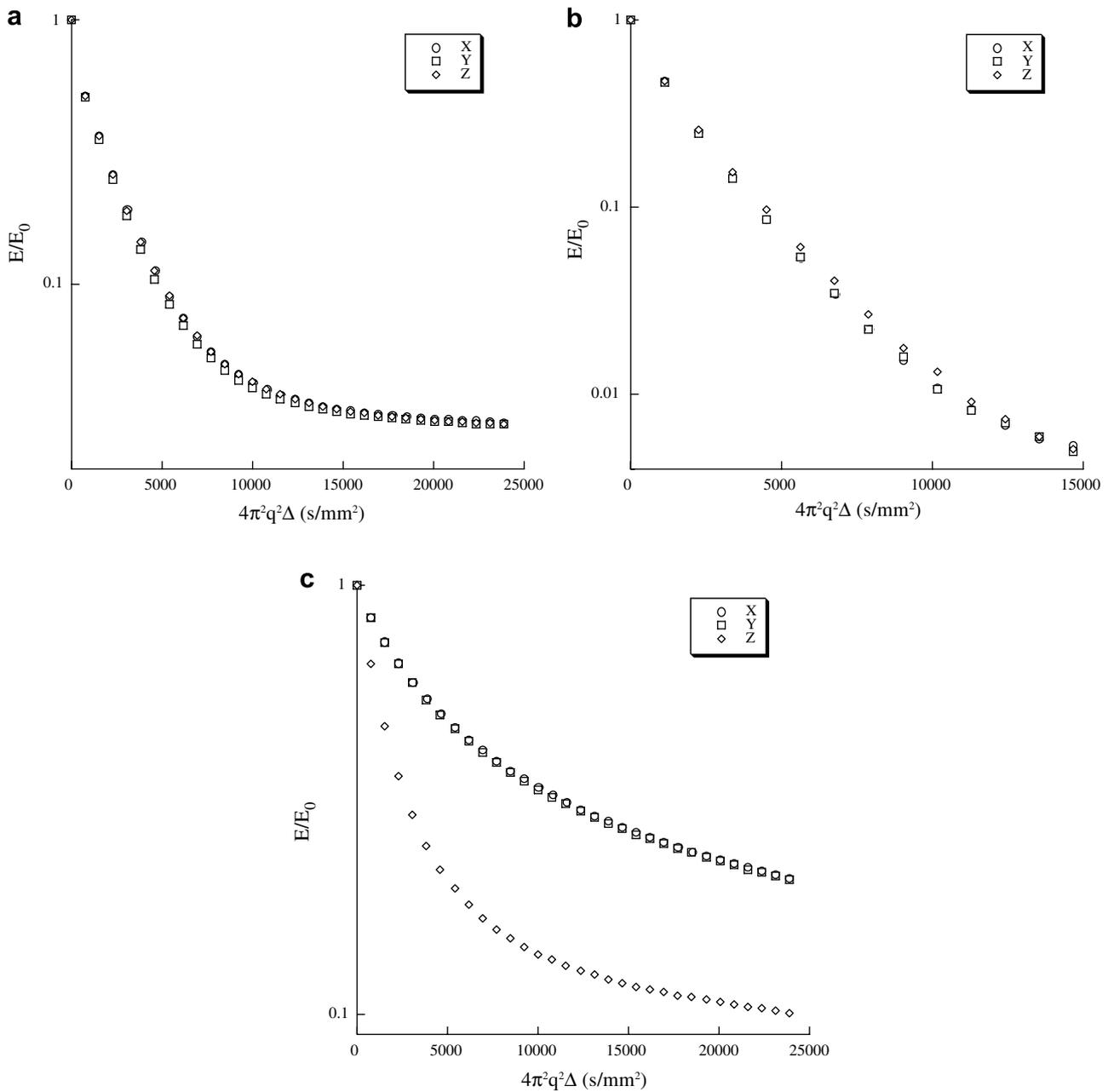
Fig. 3. Single-PGSE echo attenuation for (a) Rhesus monkey fixed cortical tissue. $\delta = 6$ ms, $\Delta = 60$ ms and $G = 400$ mT/m; (b) "Gray matter" phantom. $\delta = 6$ ms, $\Delta = 75$ ms and $G = 300$ mT/m; (c) white matter section from pig spinal cord in which the principal axis aligned in the Z direction. $\delta = 5$ ms, $\Delta = 60$ ms and $G_{max} = 400$ mT/m.

mm^2/s and $D_\perp = 0.09 \times 10^{-3}$ mm^2/s. In the higher q regime the theoretical curves deviate significantly from the observed data, which indicates that the Gaussian approximation no longer holds in this regime.

At this time, the only model of the d-PGSE echo attenuation available in the literature is the one given by Eqs. (1a) and (1b), which applies only for short diffusion times and low q values in our experiments. A more detailed model, which takes into account restricted diffusion within the tubes, is under development in our laboratory.

Fig. 5 displays the echo attenuations in the phantom resulting from the collinear and polar PGSE block combi-

nations (i.e., X_X, Y_Y, Z_Z, and X_-X, Y_-Y and Z_-Z). In theory [9], there should be no difference between the collinear and polar PGSE block combinations. The possibility of hardware artifact being the cause of the effect was ruled out as the same curves overlap (data not shown) in the isotropic samples (e.g., PDMS). This results might suggest the presence of flow in the tubes as the collinear and polar gradient combinations mimic flow compensated and uncompensated experiments [16,17]. Owing to the stability of the phantom over a 2-year period where no signal loss was observed, we ruled out exchange between the water inside the tubes and the dichlorobenzene, which

Fig. 5. Double-PGSE echo attenuation for the "gray matter" phantom in the approximately Gaussian regime. Shown are the collinear (filled symbols) and polar (open symbols) gradient combinations. $\delta = 5$ ms, $\Delta = 15$ ms, $\tau_m = 70$ ms and $G_{max} = 300$ mT/m.

Fig. 4. Double-PGSE echo attenuations, collinear (open symbols) and orthogonal (filled symbols), for the "gray matter" phantom: (a) approximate Gaussian regime experiment (symbols) and simulations (solid lines). $\delta = 5$ ms, $\Delta = 15$ ms, $\tau_m = 70$ ms and $G_{max} = 300$ mT/m; (b) restricted regime. $\delta = 3$ ms, $\Delta = 75$ ms, $\tau_m = 70$ ms and $G_{max} = 300$ mT/m.

can induce flow. A possible mechanism for that effect might originate from susceptibility differences between the fused silica tubes and the water inside. Susceptibility phenomena were a major concern during the design of the phantom. The phantom is composed of materials, which vary in their susceptibility ($\chi_{water} = -7.19 \times 10^{-7}$ cm^3/g; $\chi_{o\text{-dichlorobenzene}} = -7.48 \times 10^{-7}$ cm^3/g; $\chi_{fused\ silica} = -4.12 \times 10^{-7}$ cm^3/g) [18–20]. However, in theory the magnetic field inside an infinite cylinder is constant regardless of the susceptibility difference and the orientation with the main magnetic field [21–23]. This susceptibility difference is man-

ifested in a magnetic field shift inside each tube and depends on the tube's orientation with the magnetic field. Calculations [22] show that the frequency shift between the parallel and perpendicular tube orientation of the "gray matter" phantom is approximately 350 Hz. Indeed the line width of our phantom is 150 Hz instead of 20 Hz measured in the aligned phantom. Even though the tubes, length can be considered infinite (length/diameter = 25) we cannot rule out that variance in tube diameter and rough edges might give rise to small background gradients. However, owing to the small line width measured in the parallel phantom we believe this effect is minor.

3.3. Biological tissue d-PGSE

Fig. 6 shows the echo attenuation of d-PGSE for a fixed cortical tissue from a Rhesus monkey. The three collinear curves diverge from the six orthogonal curves, where the curves resulting from the orthogonal gradient combination experience greater attenuation than the collinear ones. As one expects, these echo attenuations are more complex than the single diameter tube phantom results presented in the previous section. It is likely that some contributions to the additional complexity in the attenuation profile arise from the large distribution in cell diameter and multiple types of cells, which constitute the gray matter tissue. The fixed cortical tissue results show microscopic anisotropy both in the low and high q regimes.

Fig. 7a shows the d-PGSE echo attenuations for fixed white matter taken from a pig's spinal cord. The data show the macroscopic anisotropy between the Z_Z and the X_X
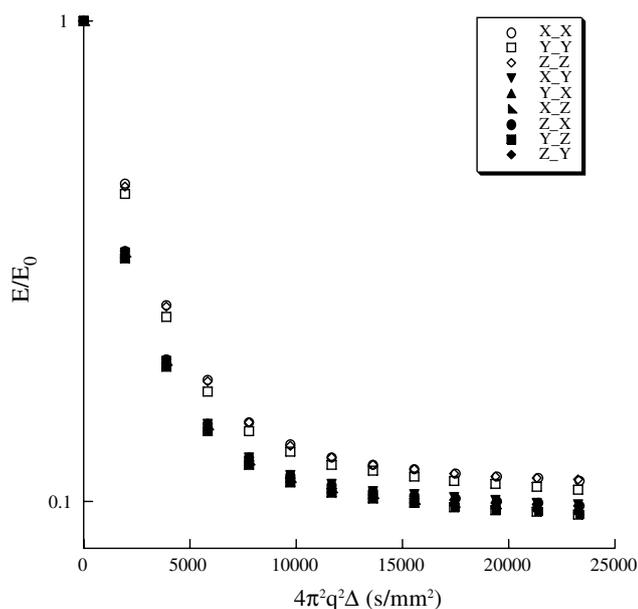
Fig. 6. Double-PGSE echo attenuation for Rhesus monkey fixed cortical tissue. $\delta = 6$ ms, $\Delta = 75$ ms, $\tau_m = 17.5$ ms and $G_{max} = 250$ mT/m.

and Y_Y direction, which was observed in the single-PGSE experiment (Fig. 4a). Additional local anisotropy in the XY plane is detected since the X_Y and Y_X direction experience greater attenuation than the collinear directions (X_X and Y_Y). This local anisotropy may result from collateral fibers that run skew to the main white matter fiber axis [24]. The polar collinear gradient combination ($X\_{-}X$, $Y\_{-}Y$ and $Z\_{-}Z$) (Fig. 7b) shows the same effect that was observed in the phantom, i.e., a greater attenuation than the collinear combination. As in the phantom, a possible mechanism for this effect is susceptibility differences within the components of the tissue. Possible sources for such differences could be the presence of micro-bubbles in the dissected tissue, differences between the susceptibility of fat (myelin) relative to water or to other membranes, or even the possible presence of residual blood clots. The complex structure of the white matter, having in it long fibers wrapped by myelin, and other non-cylindrical cells, further complicates the analysis of the results. However, we believe that susceptibility variations between those components might alter the curves only slightly, but would not create the anisotropy. The intrinsic anisotropic structure of the tissue causes the difference in the experimental attenuations.

Detecting local anisotropy, particularly in the low q regime where low gradient strengths are used and the signal-to-noise ratio is maximal, is of great interest for *in vivo* biological and clinical research studies, which are often limited by small diffusion gradients with long rise-times and limited experimental time.

This d-PGSE method can also be combined with MRI [25]. Examination of the collinear and orthogonal images could potentially reveal new information about regional anisotropy. If so, this technique could provide a new source of MRI contrast.
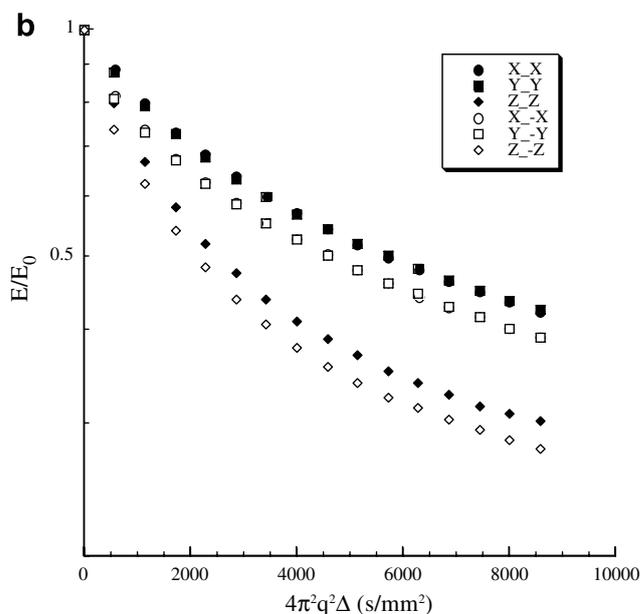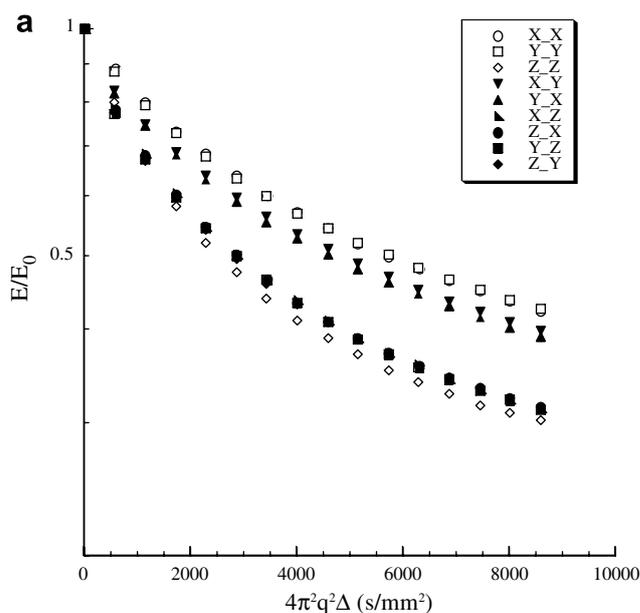
Fig. 7. Double-PGSE echo attenuation for a white matter section from pig spinal cord. $\delta = 3$ ms, $\Delta = 75$ ms, $\tau_m = 45$ ms and $G_{max} = 300$ mT/m. (a) Collinear (open symbols) and orthogonal (filled symbols); (b) collinear (filled symbols) and polar (open symbols).

In this study we used the spin echo version of the d-PGSE since both our samples (phantom and biological tissue) had sufficiently long T_2. The stimulated echo version of this sequence could be used to investigate samples that have short T_2, such as ligaments and tendon [8,16].

4. Conclusions

This experiment provides preliminary support to the hypothesis that gray matter consists of microscopic anisotropic domains that are detectable by using a multi-dimensional gradient technique such as the d-PGSE.

Local anisotropy of a "gray matter" phantom was also detected using the d-PGSE technique. For the "gray matter" phantom, simulations agree well with the experimental data when short Δ were used. In this regime the approximation of a Gaussian displacement distribution function still holds and the resulting echo attenuation is the product of the two single-PGSE experiments. For long Δ and high q values, a model which takes into account restriction and other relaxation mechanism would be more appropriate. The fixed cortical tissue results show anisotropy both in the low and high q regimes. The observation of anisotropy in the low q regime using small gradient strengths and at high signal-to-noise ratios suggests the feasibility of biological and clinical applications of d-PGSE to detect microstructure features of tissues.

Acknowledgments

References

[1] D. Le Bihan, Molecular diffusion nuclear magnetic resonance imaging, Magn. Reson. Quart. 7 (1) (1991) 1–30.

[2] C. Pierpaoli, P. Jezzard, P.J. Basser, A. Barnett, G.D. Chiro, Diffusion tensor MR imaging of the human brain, Radiology 201 (3) (1996) 637–648.

[3] P.J. Basser, J. Mattiello, D. LeBihan, Estimation of the effective self-diffusion tensor from the NMR spin echo, J. Magn. Reson. B 103 (1994) 247–254.

[4] A.R. Martin, B.G. Wallace, P.A. Fuchs, J.G. Nicholls (Eds.), From Neuron to Brain: A Cellular and Molecular Approach to the Function of the Nervous System, Sinauer Associates, 2001.

[5] E.O. Stejskal, J.E. Tanner, Spin diffusion measurement: spin echo in the presence of time-dependent field gradient, J. Chem. Phys. 42 (1) (1965) 288–292.

[6] J.E. Tanner, E.O. Stejskal, Restricted self-diffusion of protons in colloidal systems by the pulsed-gradient spin-echo method, J. Chem. Phys. 49 (4) (1968) 1768–1777.

[7] P.T. Callaghan, M.E. Komlosh, Locally anisotropic motion in a macroscopically isotropic system: displacement correlation measured using double pulsed gradient spin-echo NMR, Magn. Reson. Chem. 40 (2002) S15–S19.

[8] Y. Cheng, D.G. Cory, Multiple scattering by NMR, J. Am. Chem. Soc. 121 (1999) 7935–7936.

[9] P.P. Mitra, Multiple wave-vector extension of the NMR pulsed-field-gradient spin-echo diffusion measurement, Phys. Rev. B 51 (November 21) (1995) 15074–15078.

[10] P.T. Callaghan, S. Godfroy, B.N. Ryland, Use of the second dimension in PGSE NMR studies of porous media, Magn. Reson. Imaging 21 (2003) 243–248.

[11] P.T. Callaghan, I. Furo, Diffusion-diffusion correlation and exchange as a signature for local order and dynamics, J. Chem. Phys. 120 (8) (2004) 4032–4038.

[12] Y. Qiao, P. Galvosas, P.T. Callaghan, Diffusion correlation NMR spectroscopic study of anisotropic diffusion of water in plant tissue, Biophys. J. 89 (October) (2005) 2899–2905.

[13] P.N. Sen, Time-dependent diffusion coefficient as a probe of geometry, Concept Magn. Reson. 23A (1) (2004) 1–21.

[14] Y. Assaf, Y. Cohen, Assignment of the water slow-diffusion component in the central nervous system using q-space diffusion MRS: implications for fiber tract imaging, Magn. Reson. Med. 43 (2) (2000) 191–199.

[15] I. Ronen, K.-H. Kim, M. Garwood, K. Ugurbil, D.-S. Kim, Conventional DTI vs. slow and fast diffusion tensor in cat visual cortex, Magn. Reson. Med. 49 (2003) 785–790.

[16] A.A. Khrapichev, P.T. Callaghan, Double PGSE NMR with stimulated echoes: phase cycles for the selection of desired encoding, J. Magn. Reson. 152 (2001) 259–268.

[17] P.T. Callaghan, S.L. Codd, J.D. Seymour, Spatial coherence phenomena arising from translational spin motion in gradient spin echo experiments concept, Magn. Reson. 11 (4) (1999) 181–202.

[18] C.E. Hutchison, T. Tsang, B. Weinstock, Magnetic susceptibility of neptunium hexafluoride in uranium hexafluoride, J. Chem. Phys. 37 (3) (1962) 555–562.

[19] R.C. Wheast, Handbook of Chemistry and Physics, CRC Press, Boca Raton, FL, 1982.

[20] P.W. Kuchel, B. Chapman, W.A. Bubb, P.E. Hansen, C.J. Durrant, M.P. Hertzberg, Magnetic susceptibility: solutions, emulsions, and cells concept, Magn. Reson. 18A (1) (2003) 56–71.

[21] C. Mayer, A. Terheiden, Numerical simulation of magnetic susceptibility effects in nuclear magnetic resonance spectroscopy, J. Magn. Reson. 118 (6) (2003) 2775–2782.

[22] P.T. Callaghan, Susceptibility-limited resolution in nuclear magnetic resonance, J. Magn. Reson. 87 (1990) 304–319.

[23] D.L. VanderHart, Magnetic susceptibility & high resolution NMR of liquids & solids, in: Encyclopedia of NMR, Wiley, Chichester, 1995, 2938–2946.

[24] H. Mamata, U.D. Girolami, W.S. Hoge, F.A. Jolesz, S.E. Maier, Collateral nerve fibers in human spinal cord: visualization with magnetic resonance diffusion tensor imaging, NeuroImage 31 (2006) 24–30.

[25] M.E. Komlosh, M.J. Lizak, F. Horkay, R.Z. Freidlin, P.J. Basser, Detection of local anisotropy using double-PGSE filtered imaging, 47th ENC, Asilomar, CA (2006) E060077.